Research Article

The impact of weak inertial stimulation on visual-vestibular bimodal heading perception

Journal of Vestibular Research
2024, Vol. 0(0) 1–11

DOI: 10.1177/09574271241305019
journals.sagepub.com/home/ver

Yue Wei[1,2]*, Beisheng Bao[3]*, Jingyi Xie[1], and Richard HY So[2,3]

Abstract

Perception of self-motion involves the integration of visual and vestibular sensory information. Currently, there is limited research exploring visual-vestibular interactions under weak vestibular stimulation. This study investigates the impact of weak inertial stimulation on visual-vestibular bimodal heading perception. A translational XY-axis motion platform equipped with a 46-inch LCD TV was utilized to generate synchronized visual and inertial stimuli. The heading perception was examined under visual-only, vestibular-only, and bimodal conditions using three levels of inertial stimuli (9 mg, 14 mg, and 19 mg). In each condition, participants were tested at nine angles (±16°, ±9.2°, ±3°, ±1.7°, and 0° where 0° represents forward movement), to discern left-forward or right-forward motion. The heading discrimination threshold (HDT) was derived from participants' rightward response proportions across all angles. Our findings reveal that the HDT under 14 mg bimodal conditions is significantly higher than that under visual-only conditions (with marginal significance in the 9 mg and 19 mg conditions), indicating that the presence of weak vestibular signals might decrease the precision of bimodal heading discrimination. These results contradict the prediction of Bayesian model theory that perception is more precise under bimodal compared with unimodal conditions. The results may be explained by neurological biases during Bayesian integration, the "reduced visual precision" theory, or increased task complexity in bimodal heading discrimination. Further research with larger sample size, extending the study to varied inertial stimuli and visual coherence levels, will be beneficial for clarifying its underlying mechanisms.

Keywords

heading, threshold, visual-vestibular integration, self-motion

Received: 28 May 2024; revised: 6 November 2024; accepted: 13 November 2024

Introduction

Accurately discriminating the direction of self-motion, or heading direction, is essential for humans in various activities,[1,2] including walking, driving, and controlling remote unmanned vehicles. Humans possess the ability to integrate sensory information from multiple modalities to perceive heading direction, with visual and vestibular cues playing pivotal roles.[3–8] Visual cues, such as optic flow, provide heading information by referencing the surrounding objects.[9–11] Simultaneously, the vestibular system detects the head's inertial motion, contributing to heading perception.[12–14] Exploring the integration of visual and vestibular information not only helps us understand how humans achieve heading perception but also enhances our understanding of human multisensory integration processes. Research on the simultaneous utilization of visual and vestibular cues in heading perception and the underlying mechanisms governing their integration is receiving increasing attention.[3,4,6,15–21]

According to current behavioral and neurological findings,[1,5,6,22–26] the concurrent presence of both visual and vestibular cues generally enhances heading discrimination performance compared to conditions involving either modality alone. Recent studies have provided new evidence that further supports the notion that visual and vestibular

[1]Department of Basic Psychology, School of Psychology, Shenzhen University, Shenzhen, China
[2]HKUST-Shenzhen Research Institute, Shenzhen, China
[3]Department of Industrial Engineering and Decision Analytics, The Hong Kong University of Science and Technology, Hong Kong, China

*These authors contributed equally to this work.

Corresponding author:
Yue Wei, Department of Basic Psychology, School of Psychology, Shenzhen University, 3688 Nanhai Avenue, Nanshan District, Shenzhen 518060, China; HKUST-Shenzhen Research Institute, 9 Yuexing First Road, South Area, Hi-Tech Park, Nanshan, Shenzhen 518057, China.
Email: yweiaj@szu.edu.cn

information combine in a statistically optimal manner.[1,2,5–8,23,27,28] By utilizing Bayesian integration, the reliability and precision of both visual and vestibular modalities can be effectively combined, resulting in a statistically optimal estimation of heading direction. The variance of optimal bimodal heading discrimination, which integrates visual and inertial cues, can be predicted based on the variance of unimodal heading discrimination using either visual cues alone or inertial cues alone.[5,6,22] The predictive equation (equation (1)) is the following:

$$\sigma_p^2 = \frac{\sigma_{ve}^2 \sigma_{vi}^2}{\sigma_{ve}^2 + \sigma_{vi}^2} \quad (1)$$

where the heading discrimination threshold (HDT) quantifies the variance of heading perception (smaller HDT indicates more precise and reliable heading discrimination performance), σ_p is the predicted bimodal HDT, σ_{ve} is the HDT with inertial cues alone, and σ_{vi} is the HDT with visual cues alone.

An important point to note is that most of existing empirical studies only explored supra-threshold vestibular signals induced by large magnitudes of translational motion that well surpassed the otolith threshold for detecting translational motion.[1,6,22,29] The principle of visual-vestibular integration, which states that bimodal integration of visual and vestibular cues is superior to both unimodal cues, has not been examined under conditions of low vestibular reliability, particularly in near-threshold conditions, where the translation magnitude is relatively small and close to the threshold of what the otoliths can sense translational motion. In recent years, some studies on multisensory integration[30–34] have revealed that cross-modal integration mechanisms also exist for sub-threshold information across modalities (such as visual and auditory information and visual and olfactory information). Sub-threshold or unconscious cross-modal stimuli can affect participants' task performance.[30,31,35] Therefore, further research on how weak vestibular stimulation influences bimodal heading perception of visual-vestibular cues can reveal visual-vestibular integration mechanisms at the near-threshold level, offering additional evidence for multisensory information integration.

In summary, this study aims to explore the impact of weak vestibular stimulation on visual-vestibular bimodal heading perception. Specifically, we will assess differences in bimodal HDTs (visual and vestibular stimuli) compared to unimodal HDTs (visual-only and vestibular-only) under a range of weak vestibular stimulations.

Methods

Participants

A total of 10 participants (age: 23.88±1.27; male/female: 8/2) were recruited for this study. The sample size was selected based on similar studies in the field.[1,21,22,29,36] All participants voluntarily signed a consent form indicating their willingness to participate. All participants had normal vision or vision corrected to normal using the Stereo Optical Co. Inc. Vision Tester (Model 2000). They were instructed to abstain from consuming alcohol and caffeine beverages for 10 hours prior to the experiment. Participants with a history of vestibular disease or lesions, high susceptibility to motion sickness, or any visual system-related diseases or injuries were not included. Based on previous research,[37] participants scoring above the 70th percentile on the Motion Sickness Susceptibility Questionnaire (MSSQ)[38] were excluded from the study due to the likelihood of experiencing severe motion sickness symptoms. They were unaware of the specific objectives of the experiment and were not undergoing any medical treatment during the study period. Participants were compensated with 50 HKD per hour for their participation. The study adhered to the ethical requirements set by the University Research Ethics Committee and followed the guidelines outlined in the Declaration of Helsinki. Approval for the study was obtained from the Human Participants Research Panel of the Hong Kong University of Science and Technology (HKUST).

All participants who took part in the experiment underwent a training and screening session lasting approximately 1 h. During this session, they were exposed to all the heading stimuli used in the main experiment. To keep the quality of the data, participants who fulfilled the following requirements were included in the formal experiment: firstly, subjects should confirm that they fully understood the experiment procedure; secondly, subjects should be capable to follow the instructions and make response within required time; thirdly, subjects did not report severe symptoms of motion sickness. One subject did not pass the screening as he did not response within the specified time (5 s) for more than 5% of trials. None of the participants reported experiencing noticeable symptoms of motion sickness. The remaining nine participants successfully completed the formal experiment, and their data was analyzed and presented in this paper.

Apparatus

Inertial stimulation apparatus. A translational XY-axis motion platform (Figure 1(a)) was employed to generate inertial heading cues. This platform was constructed at the China Light & Power (CLP) Power Wind/Wave Tunnel Facilities of HKUST and featured a fully enclosed testing platform measuring 4 m × 3 m. To ensure stability, the platform was supported by precisely machined rails and custom sliding bearings. It had the capability to move along the fore-and-aft axis (x) and lateral axis (y) by utilizing an electromagnetic actuation mechanism for power (see additional information in Appendix I.1).

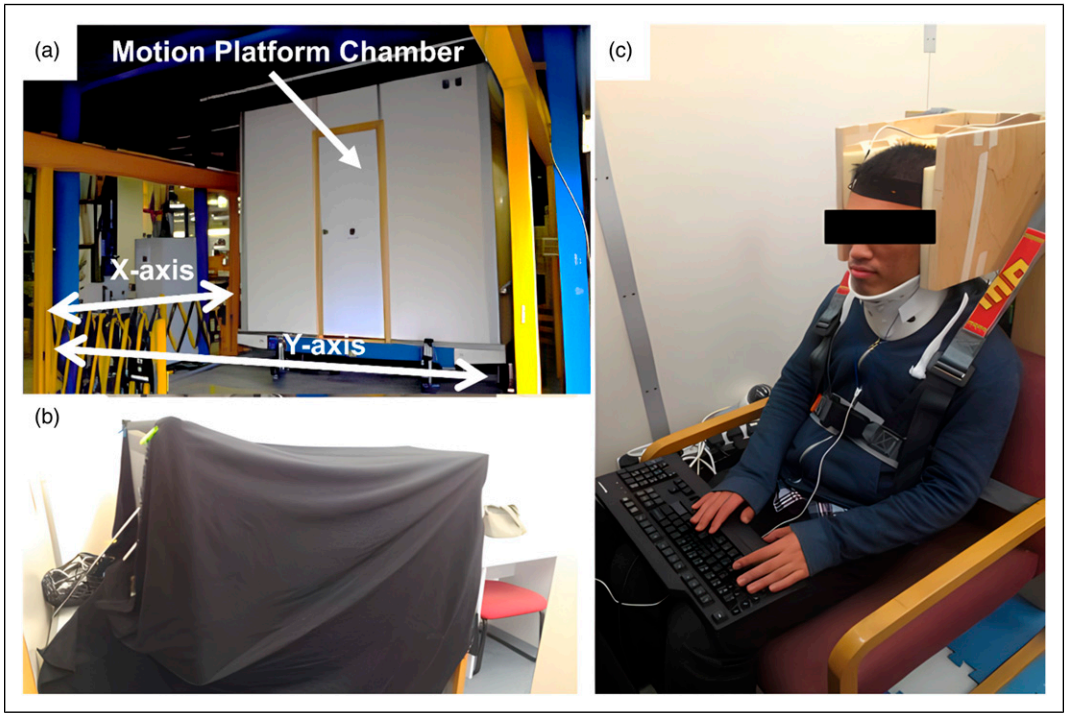

Figure 1. Motion platform and three types of motion stimuli. Apparatus used in the experiment (a) translational XY-axis motion platform at the CLP Power Wind/Wave Tunnel Facilities of HKUST, (b) subject and the LCD TV enclosed by a black curtain, and (c) subject sitting on a chair with back and head rests. The subject responses were reported using a keyboard. Body and head movements were restricted by a 4-point harness, chin rest, and two wooden panels.

Visual stimulation apparatus. A 46-inch LCD TV was installed within the motion platform to provide visual heading stimuli. This TV was securely mounted on a steel-framed cabinet to ensure stability during motion platform movements (Figure 1(b)). A chair equipped with a backrest and headrest was placed in front of the TV on foamed plastic to minimize vibration noise and align the seated subject's eye level with the center of the TV screen (Figure 1(c)). The chair was positioned at 70 cm from the TV, providing the subject with a field of view (FOV) of 80° horizontally and 45° vertically. The TV had a resolution of 1920 × 1080 pixels and a refresh rate of 60 frames per second.

The vestibular stimuli and visual stimuli were synchronized with calibration using a control program linked to an accelerometer, with a maximum error not exceeding 50 ms, which is acceptable based on previous work.[36]

Control setups. Subject movement was restricted using a 4-point harness, and head motion was controlled with a medical chin rest and wooden panels on either side of the headrest, with sponges filling any gaps. Accelerometers were attached to both the chair and a head belt to monitor inertial and head movements, respectively. The setup ensured comfort without allowing independent body movement during the motion platform's operation (Figure 1(c)). Subjects indicated their perceived heading directions using a keyboard. The control and display software were programmed using OpenGL and C++. To mitigate auditory cues from the motion platform, which produced noise around 55 dBA, a 75 dBA white noise was played through ear canal headphones. The motion platform chamber was isolated with the door closed, lights off, and was surrounded by a black curtain to eliminate environmental influences (see Figure 1(b) and (c)).

Testing protocols

Inertial stimuli. In this study, a 5-second inertial stimulus was employed with a uni-directional linear motion, characterized by a 0.2 Hz sinusoidal acceleration profile (see Figure 2). Following each inertial stimulus, the motion platform executed a "homing" motion to return to its starting point, employing a motion profile similar to the initial stimulus but in the reverse direction. Before the start of each formal trial, there was a "beep" sound, indicating the beginning of the trial. When a response was required from the participant, text prompts appeared on the screen. Subjects were given instructions to ignore the direction of the homing motion and provide their perceived heading direction prior to the initiation of the homing motion. During homing motion, text prompts of "do not answer" appeared on the screen, which reminded participants to ignore the motion. This rendered

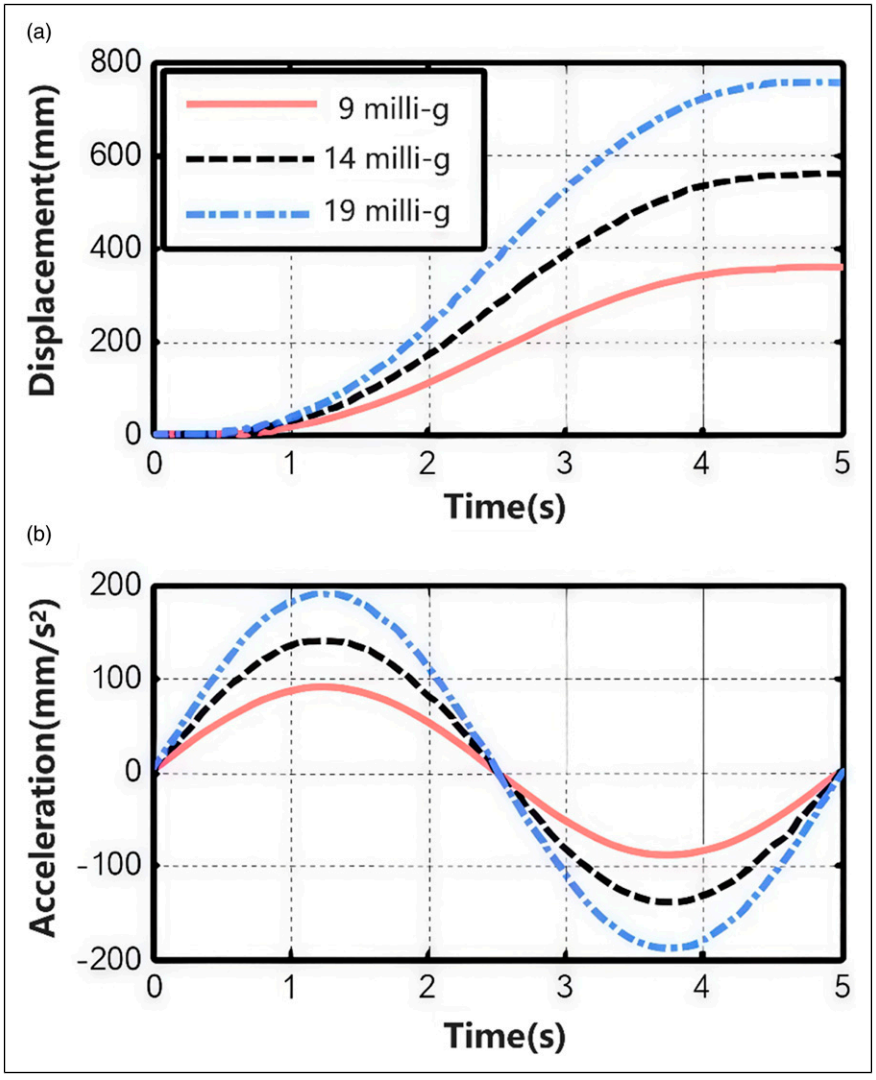

Figure 2. Motion profile for inertial stimuli. (a) The displacement profile of the inertial motion. (b) The corresponding acceleration profile. Inertial stimuli are indicated by peak accelerations of 9 mg (solid red line), 14 mg (dashed black line), and 19 mg (dot-dash purple line).

any responses given during the homing motion as invalid and not considered for analysis.

To evaluate the influence of weak inertial stimuli, we employed three different levels of peak acceleration: 9 mg, 14 mg, and 19 mg. Each acceleration level was tested in nine different directions: ±16°, ±9.2°, ±3°, ±1.7°, and 0°. The reference angle of 0° corresponded to the direction of the subject directly facing forward. Positive angles indicated motion toward the subject's right side, while negative angles indicated motion toward the left side.

In this study, "near-threshold" refers to stimuli that are close to the translational inertial stimuli just adequate for distinguishing lateral (left or right, ±90-degree headings) translational motion. Based on our previous research using the same equipment, motion profile, and participant group, the average inertial linear translation direction-recognition threshold at around 0.2 Hz is 10 ± 1.39 mg.[37] Therefore, the smallest inertial motion stimulus selected for this study (9 mg) is near this measured threshold, while the maximum peak acceleration of 19 mg represents the highest level achievable at 0.2 Hz with our motion platform. The three inertial motion stimuli (9/14/19 mg) selected for this study cover a specific range of weak translational inertial stimuli.

Visual stimuli. In our experiment, we utilized a 5-second visual stimulus featuring a zooming star-field composed of 900 small white spheres against a black background, simulating an observer's inertial motion through space. These spheres, randomly positioned but evenly distributed, would appear to move toward the observer and then disappear, with adjustments made to prevent the spheres from appearing excessively large as they approached. The field of

view (FOV) for the visual stimuli was set to match the LCD TV's FOV at 80° × 45°. A red fixation cross was placed at the center of the screen, and subjects were instructed to focus on it under all conditions, including those with only inertial cues. To enhance the stimulus' impact and consider the frequency response of vection, which is most responsive in the low-frequency range of 0.1–0.2 Hz, we applied a 0.2 Hz frequency.[39,40]

We chose an 8% visual coherence for the stimuli, meaning that only 72 of the spheres moved in a coherent manner, reflecting the experiment's aim to reduce the overall strength of the visual stimulus. This approach ensures that in bimodal conditions—where visual and inertial motions are synchronized and headed in the same direction—the visual perception isn't overwhelmingly dominant, allowing for a more balanced comparison across conditions. The chosen level of coherence was based on previous research findings. Studies have demonstrated that visual heading discrimination performance remains high with dot cloud stimuli ranging from 10 to 63 dots.[10] Additionally, subjects have been able to discriminate a divergence optical flow of approximately 20 dots from noise dots.[41,42] This experimental setup was designed to attain a visual heading discrimination threshold (HDT) that is comparable to the vestibular HDT achieved with a peak acceleration of 19 mg. The selection of the visual stimulus was made to ensure the provision of a valid and effective visual cue, while also ensuring that the reliability of information in both modalities (visual and vestibular) was relatively similar.

Heading discrimination threshold (HDT). The heading discrimination threshold (HDT) has been widely used in previous research studies[1,5,22–24] and was used in this study as well, to assess heading perception precision and reliability. The HDT represents the standard deviation of the perceived heading direction, which follows a normal distribution centered on the stimulus's heading angle (see Figure 3 for detail). To measure this, a heading discrimination task was developed, requiring subjects to determine if the motion direction was to the left or right of a forward-facing zero degree. The smallest angle deviation at which subjects could accurately identify the heading direction with at least an 84% correct rate was defined as the HDT (Figure 3).

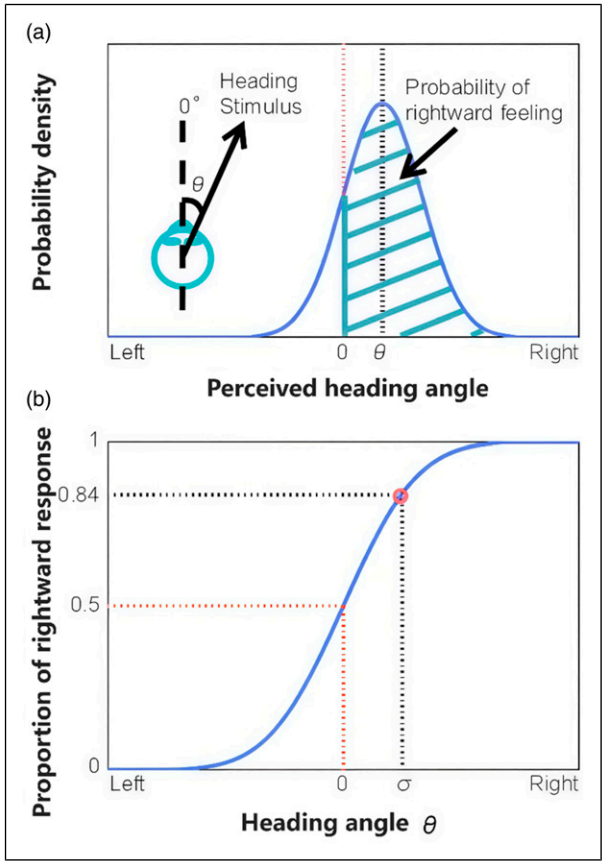

Figure 3. The fitted normal distribution for heading discrimination threshold (HDT) calculation. (a) The illustration for the distribution of the heading angle perception. The subject's facing direction is considered as 0°, and the angular deviation of the heading stimulus is denoted as θ. The perceived heading angle follows a normal distribution N (θ, σ). The shaded area between 0 and positive infinity represents the probability of perceiving a rightward heading direction. (b) The calculation of HDT. During the experiment, the subject is exposed to multiple heading stimuli, and after each exposure, they report their perceived direction. Through this repeated exposure-report procedure, the proportion of rightward responses can be calculated. By analyzing the proportion of rightward responses reported by the subjects, a normal distribution can be fitted to the data. The mean of this distribution represents the 0.5 proportion point, indicating the average perceived heading direction. The standard deviation (σ) corresponds to the 0.84 proportion point, which is defined as HDT (the variance of the perception distribution).

Experiment procedure. In this experiment, there are two levels for visual stimuli (on or off) and four levels for vestibular stimuli (off, 9 mg, 14 mg, and 19 mg). Hence, the study involved testing seven conditions (see Table 1): one visual-only condition (Vis), three vestibular-only conditions with different inertial stimuli (Ves9, Ves14, and Ves19), and three combined conditions with both visual stimuli and different inertial stimuli (Com9, Com14, and Com19).

In each condition, there were a total of 270 trials. These trials were divided into three blocks, with each block consisting of 90 trials. The presentation order of the trials within each block was randomized. Each participant completed a total of seven experiment sessions, with each session consisting of one experimental condition and lasting 1 hour. Therefore, each participant completed a total of 270 × 7 = 1890 trials. Within each session, there were three blocks of trials. A 5-minute rest period was provided between every two blocks to prevent fatigue. The seven experimental sessions were conducted on different days in a random order to minimize the potential influence of motion

Table 1. Experiment design with visual stimuli and inertial stimuli.

Visual stimuli	Inertial stimuli magnitude (mg)				
	On	Off	9	14	19
		Vis	Com9	Com14	Com19
	Off	NA[a]	Ves9	Ves14	Ves19

× 9 heading (degree): −16 (left), −9.2, −3, −1.7, 0, 1.7, 3, 9.2, 16 (right)
× 30 repetitions (3 blocks)

[a]NA, not applicable. The condition with no visual and inertial cues was not tested as it is not relevant to current study. The reference angle of 0° corresponded to the direction of the subject directly facing forward. Positive angles indicated motion toward the subject's right side, while negative angles indicated motion toward the left side.

sickness aftereffects and fatigue. Participants were forced to choose either left or right via keyboard trial-by-trial. Missed trials occurred if participants did not respond within the specified time. Participants with more than two misses in a session (about 1% missing rate) would repeat the session on another day to keep the quality of the data.

Subjects completed pre- and post-exposure Simulator Sickness Questionnaires (SSQ)[43] before and after each session to monitor participants' motion sickness levels. Subsequently, the participants took part in a brief interview where they were asked whether they detected forward motion, how many motion stimuli onsets they detected during one trial, and if they experienced any other special sensations.

Data analysis

Firstly, the rightward response proportion for nine heading directions (±16°, ±9.2°, ±3°, ±1.7°, and 0°) was calculated under all seven conditions (Vis, Ves9, Ves14, Ves19, Com9, Com14, and Com19). Given that weak inertial motions were used, it is possible that subjects were unable to discriminate the linear translation heading directions (specifically, distinguishing left-forward from right-forward) in this study. If there was no significant difference in the response proportion between heading stimuli with rightward and leftward heading directions, the HDTs would be either infinity or values with large fitting error. To confirm discrimination capability and conditions that proper for HDT calculation, we conducted Wilcoxon rank sum tests comparing the proportion of response between left-forward and right-forward heading directions. If the subjects show significant differences in any one of the four pairs of angles (±16°, ±9.2°, ±3°, and ±1.7°), we consider them to have passed the discrimination test.

Subsequently, we calculated the HDT only for conditions and subjects that passed the discrimination capability tests. For each condition and each subject, based on the rightward response proportion for the nine heading directions, we utilized Matlab's Psignifit 3.0 toolbox to fit the data using a cumulative normal distribution. After obtaining the fitted curve, we could derive the HDT (the variance of the perception distribution) by determining the standard deviation (σ) corresponding to the 0.84 proportion point on the curve according to the definition of HDT.

Finally, we examined whether there were differences in HDT between visual unimodal (Vis) and three bimodal conditions (Com9, Com14, and Com19). All statistical analyses were performed using SPSS 24.0. Initially, we conducted a Shapiro–Wilk test to assess if the data followed the normal distribution. For data that passed the normality test, we applied paired-sampled t-tests. If the data did not pass the normality test, we employed paired Wilcoxon signed rank tests. Additionally, we utilized the same approach to assess whether there were differences in HDT between different bimodal conditions.

Results

Discrimination capability examination

Wilcoxon rank sum tests demonstrated that all participants could significantly distinguish stimuli moving to the left-forward from those moving to the right-forward ($p < 0.05$) in the visual cues condition (Vis) and the combined cues conditions (Com9, Com14, and Com19). For the Ves14 condition, three participants could significantly distinguish left-forward motion from right-forward motion ($p < 0.05$), while for Ves19, four participants passed the discrimination capability tests ($p < 0.05$). However, no significant discrimination was observed in the Ves9 condition for all subjects, indicating that the inertial stimulation (9 mg) in this condition was below the threshold of discrimination perception for the participants.

Post-experiment interviews revealed that all subjects detected forward motion in the Ves9 condition, suggesting it was just above their detection threshold. Since participants were unable to distinguish different heading directions under the Ves9 condition, this condition was not included in the subsequent analysis of HDT.

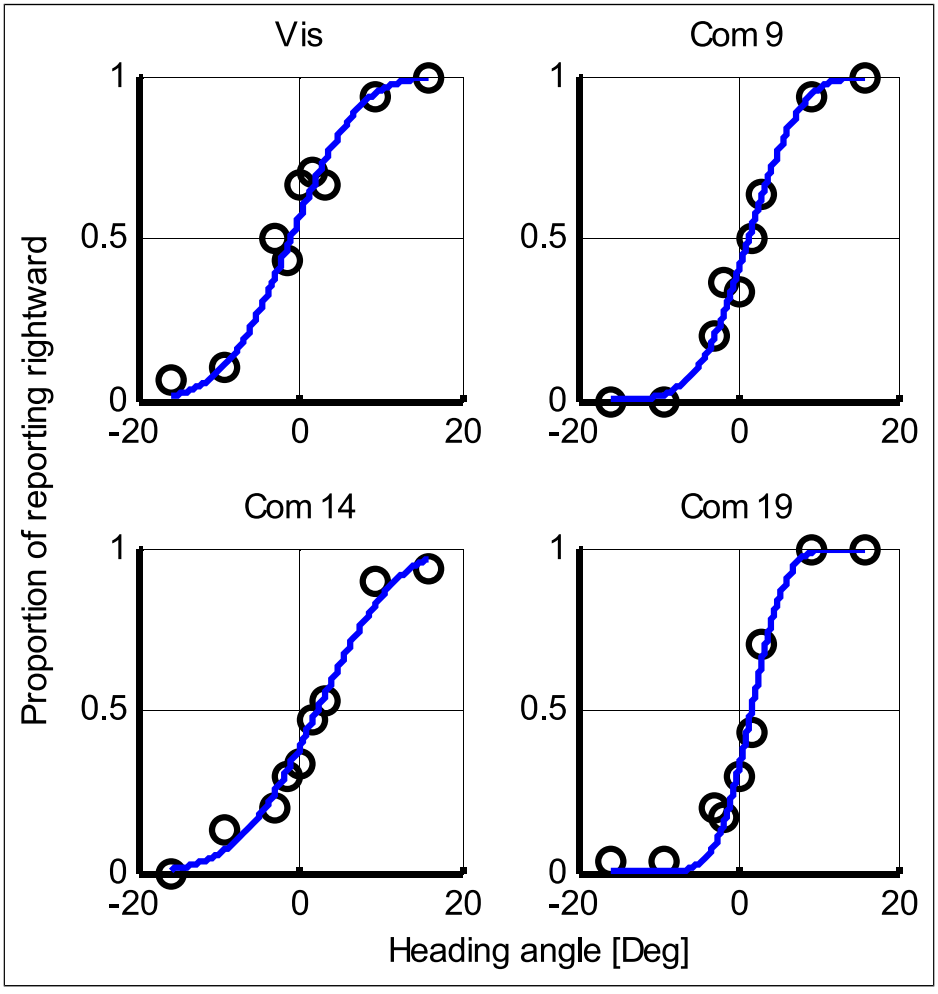

Figure 4. Sample subject response data with fitted cumulative normal distribution. Sample subject (No. 1) data on rightward response proportion (black circle) and fitted cumulative normal distribution (blue curve) for HDT calculation in visual and combined conditions. Vis, visual-only condition; Com 9/14/19, three combined conditions (Com9, Com14, and Com19) with both visual stimuli and different inertial stimuli (9/14/19 mg).

Heading discrimination thresholds (HDTs)

Using the rightward response proportion for the nine heading directions, we employed Matlab's Psignifit 3.0 toolbox to fit the data using a cumulative normal distribution (see Figure 3 for illustration and Figure 4 for sample data). This allowed us to derive the heading discrimination thresholds (HDTs) for the six conditions (Vis, Ves14/19, and Com9/14/19) that passed the discrimination capability tests.

As the vestibular stimuli were weak, a certain number of participants were unable to discriminate the direction under the inertia-only stimuli of Ves14/Ves19, making calculation of the HDT impossible. In the Ves14 condition, only 3 participants (33.3% of the sample) were able to measure the HDT accurately. In the Ves19 condition, 4 participants (44.4% of the sample) were able to measure the HDT. The mean and standard deviation (SD) of vestibular HDTs were as follows: (i) 14 mg vestibular HDT ($n = 3$): 49.32° ± 28.94°; (ii) 19 mg vestibular HDT ($n = 4$): 43.36° ± 21.40°.

In the visual and combined conditions, all participants were able to distinguish the direction, and the HDT was successfully calculated for all of them. The mean and SD of visual and bimodal HDTs were as follows (see Figure 5 for box plot of the data): (i) visual HDT = 6.87° ± 2.56°; (ii) 9 mg bimodal HDT = 16.48° ± 12.91°; (iii) 14 mg bimodal HDT = 15.19° ± 14.56°; and (iv) 19 mg bimodal HDT = 11.53° ± 6.95°. Figure 5 shows the box plots of the heading discrimination thresholds (HDTs) for the visual condition (Vis) and the combined conditions (Com9, Com14, and Com19) for all participants.

Comparing unimodal and combined conditions

Firstly, we compared the differences between the visual and bimodal HDTs. Among all the conditions, only the

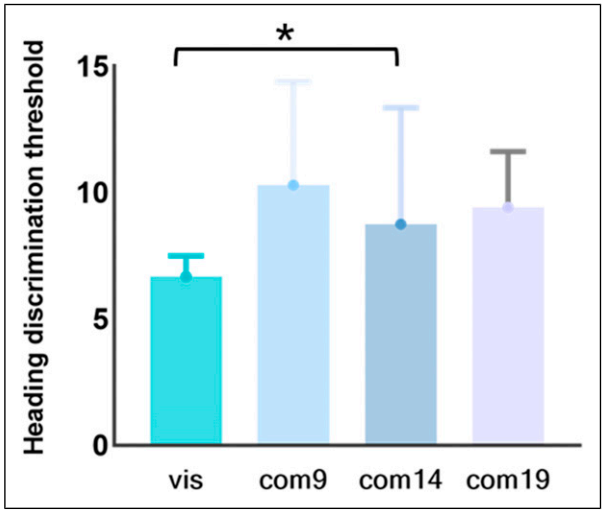

Figure 5. Median and SEM for HDTs in visual and combined conditions. * $p < 0.0167$ (with Bonferroni corrected for multiple tests). HDT: heading discrimination threshold; Vis: visual-only condition; Com 9/14/19, three combined conditions (Com9, Com14, and Com19) with both visual stimuli and different inertial stimuli (9/14/19 mg). Note: HDTs for Com14 did not pass the normality test (Shapiro–Wilk test, $p < 0.01$). Paired Wilcoxon signed rank tests were used for Com14, while paired sample t-tests were applied for other conditions.

HDTs of Com14 failed the normality test (Shapiro–Wilk test, $p<0.01$). Consequently, for the Com14 condition, pairwise hypothesis testing was conducted using paired Wilcoxon signed rank tests, while for the other conditions, paired sample t-tests were used. The Bonferroni correction was applied, and the significance threshold was readjusted to $0.05/3 = 0.0167$ to account for the three comparison tests. Results showed that visual HDT is only significantly smaller than 14 mg bimodal HDT (Wilcoxon signed rank tests, $p = 0.008$), and marginal significantly smaller than 9 mg bimodal HDT ($t(8) = -2.434$, $p = 0.041$) and 19 mg bimodal HDT ($t(8) = -2.373$, $p = 0.045$). Although there was an increase in the number of participants for whom HDTs could be measured as the intensity of the inertial stimulation increased, the differences between the different conditions were not statistically significant. The results suggest that in the 14 mg condition, the presence of congruent but weak vestibular signals seemed to weaken an individual's ability to discriminate heading direction.

Given the weak nature of the inertial stimuli, the vestibular unimodal HDT could only be measured for 33%–44% of participants, a proportion much lower than that under bimodal conditions (where HDT can be measured for all participants). Moreover, the mean values of the measured HDTs were notably higher compared to those recorded under the combined conditions. This indicates that bimodal heading perception was enhanced with combined visual information in contrast to weak vestibular unimodal conditions.

Validation

Simulator Sickness Questionnaire (SSQ) scores were significantly higher than zero across all conditions (Wilcoxon signed rank test, $p < 0.05$) but showed no significant correlation with HDTs (Pearson's r = 0.29, $p>0.05$) nor differences across conditions (see Appendix 2I.2 for SSQ scores), suggesting that motion sickness did not significantly impact the results.

To assess the repetition's influence on fitted HDTs, we calculated HDTs with 10, 20, and 30 repetitions in the Vis, Com9, Com14, and Com19 conditions (see Appendix 3I.3 for repetition effect on HDTs). No significant differences were found between HDTs from 10, 20, and 30 repetitions in all four conditions (Wilcoxon signed rank test, $p > 0.05$).

The results of the brief interview conducted after the experiment showed that all subjects could detect forward motion under all conditions. All participants only detected one motion onset during one trial, and none of the participants mentioned detecting two separate stimuli onsets for visual and vestibular stimuli.

Discussion

This study investigates the pattern of visual and vestibular information integration when inertial signals are consistent with visual information but weak for direction discrimination. The results indicate that the integration of multimodal information does not always enhance perceptual precision. In this section, we discuss three main topics: (1) Bayesian predictions bias, (2) other possible explanations, and (3) limitations and future work.

Bayesian prediction bias

This study found that the presence of weak vestibular signals seemed to decrease the performance of heading discrimination, which contradicts the predictions of Bayesian model theory. According to Bayesian model theory,[1,2,5,8,22] the addition of extra inertial cues enhances heading discrimination performance and is typically beneficial. However, the experimental results revealed that bimodal HDTs at 14 mg condition were significantly higher than visual-only HDTs, indicating that adding vestibular cues did not always lead to improved heading perception.

These results might be explained by the neurological prediction bias proposed by previous works. It has been observed that in some conditions, the performance of bimodal heading discrimination deviates significantly from the optimal predictions of Bayesian inference.[6,23,24,29] It is suggested that the observed prediction bias is primarily

caused by an overweighting of the vestibular signal, leading to the term "vestibular overweighting."[6,23,29] In fact, in the few subjects where HDT could be measured, the Bayesian predicted bimodal HDT derived from equation (1) was also smaller than the measured bimodal HDT (see Supplemental documents for analysis), which is consistent with the bias reported by previous works.[6,23,24,29]

Other possible explanations

Another potential explanation for our findings is the "reduced visual precision" theory proposed by De Winkle et al.,[44] which suggests that visual sensitivity declines when exposed to inertial motion, leading to a prediction bias. According to previous research on neurological response of visual-vestibular interactions,[7,45–48] the activities of visual cortex can be suppressed when subjects are exposed to both visual and vestibular stimuli.[45,49,50] As a result, the precision of visual heading discrimination may be compromised by non-conflicting weak inertial cues. Some recent studies also demonstrated that the inclusion of congruent visual information can diminish the accuracy of vestibular perception,[20,51] which is consistent with our results.

Another possibility is that the increased complexity and difficulty of the bimodal heading discrimination task required participants to divide their attention between visual and inertial cues. In bimodal conditions, less attention may be directed toward visual cues compared to the visual-only condition, while the inertial cues are insufficient to compensate for the loss in visual heading discrimination precision. As a result, higher bimodal HDTs were observed compared to visual HDTs.

Limitations and future work

This study focuses on exploring weak and near-threshold vestibular signals, which are stimuli close to translational inertial stimuli just sufficient for discerning lateral (left or right, ±90-degree headings) translational motion. Consequently, within this range, many participants were unable to measure the vestibular unimodal HDT. Future research could consider investigating a wider range of peak acceleration and motion frequencies, offering additional insights and further elucidating the mechanisms of visual-vestibular interaction in heading perception.

Furthermore, this study only investigated the visual-vestibular integration mechanisms under the fixed visual condition of 8% visual coherence. To reveal the mechanisms near the threshold, it would be beneficial to include visual conditions with varying levels of reliability. By incorporating a range of visual coherence values, further research can provide a more comprehensive and accurate understanding. Measuring bimodal HDTs across different levels of visual coherence could be considered in future studies.

Stimulus frequency is another factor to consider. The 0.2 Hz frequency used in this study is lower than previous studies, resulting in longer stimulus durations. This increased duration may contribute to greater fatigue among participants. The effects of longer stimulus duration or lower stimulus frequency on HDT and visual-vestibular integration remain unknown and require further investigation in future research.

Additionally, the relatively small sample size in this study is another limitation that warrants attention. This could lead to insufficient statistical power, potentially resulting in marginally significant findings in certain conditions. Increasing the sample size in future studies to validate the current research findings is essential.

Conclusion

This study provides evidence indicating that non-conflicting weak inertial motion cues at 14 mg can lead to larger bimodal heading discrimination thresholds (HDTs) as compared to visual unimodal conditions. The results could be explained by several possibilities, including the prediction bias in Bayesian prediction, the "reduced visual precision" theory proposed by De Winkle et al.[44] and the increased difficulty of the bimodal heading discrimination task. Further research is needed to clarify its underlying mechanisms. Expanding this research with a larger sample size and exploring different levels of visual coherence and inertial stimulus will enhance our understanding of bimodal heading discrimination.

Acknowledgments

The authors wish to thank Dr Du Bo for technical support.

Declaration of conflicting interests

The author(s) declared no potential conflicts of interest with respect to the research, authorship, and/or publication of this article.

Funding

The author(s) disclosed receipt of the following financial support for the research, authorship, and/or publication of this article: The authors would like to thank the National Natural Science Foundation of China under project No. 32200923 and Shenzhen Science and Technology Innovation Committee for partially supporting the work via project No. 20220810172237002 and No. 20231124100927001. This research is also partially supported by the Hong Kong Research Grants Council through 619210 and 618812.

ORCID iD

Yue Wei https://orcid.org/0000-0002-3766-4025

Supplemental Material

Supplemental material for this article is available online.

References

1. Butler JS, Smith ST, Campos JL, et al. Bayesian integration of visual and vestibular signals for heading. *J Vis* 2010; 10(11): 1–13.
2. Hou H and Gu Y. Multisensory integration for self-motion perception. In: *The senses: a comprehensive reference*. Amsterdam: Elsevier Science, 2020, pp. 458–482.
3. Benson AJ and Brown SF. Visual display lowers detection threshold of angular, but not linear, whole-body motion stimuli. *Aviat Space Environ Med* 1989; 60(7): 629–633.
4. Telford L, Howard IP, and Ohmi M. Heading judgments during active and passive self-motion. *Exp Brain Res* 1995; 104(3): 502–510.
5. Gu Y, Angelaki DE, and DeAngelis GC. Neural correlates of multisensory cue integration in macaque MSTd. *Nat Neurosci* 2008; 11(10): 1201–1210.
6. Butler JS, Campos JL, and Bülthoff HH. Optimal visual–vestibular integration under conditions of conflicting intersensory motion profiles. *Exp Brain Res* 2015; 233(2): 587–597.
7. Zhou L and Gu Y. Cortical mechanisms of multisensory linear self-motion perception. *Neurosci Bull* 2023; 39(1): 125–137.
8. Jerjian SJ, Harsch DR, and Fetsch CR. Self-motion perception and sequential decision-making: where are we heading? *Philos Trans R Soc Lond B Biol Sci* 2023; 378(1886): 20220333.
9. Gibson JJ. *The perception of the visual world*. Houton, TX, Boston, FL: Mifflin, 1950.
10. Warren WH, Morris MW, and Kalish M. Perception of translational heading from optical flow. *J Exp Psychol Hum Percept Perform* 1988; 14(4): 646–660.
11. Lappe M, Bremmer F, and Van den Berg AV. Perception of self-motion from visual flow. *Trends Cognit Sci* 1999; 3(9): 329–336.
12. Guedry FE. Psychophysics of vestibular sensation. In: HH Kornhuber (ed) *Handbook of sensory physiology, The vestibular system*. New York, NY: Springer, 1974.
13. Benson AJ, Spencer MB, and Stott JR. Thresholds for the detection of the direction of whole-body, linear movement in the horizontal plane. *Aviat Space Environ Med* 1986; 57: 1088–1096.
14. MacNeilage PR, Banks MS, DeAngelis GC, et al. Vestibular heading discrimination and sensitivity to linear acceleration in head and world coordinates. *J Neurosci* 2010; 30(27): 9084–9094.
15. Ohmi M. Egocentric perception through interaction among many sensory systems. *Cognit Brain Res* 1996; 5(1-2): 87–96.
16. Harris LR, Jenkin M, and Zikovitz DC. Visual and non-visual cues in the perception of linear self motion. *Exp Brain Res* 2000; 135(1): 12–21.
17. Dokka K, DeAngelis GC, and Angelaki DE. Multisensory integration of visual and vestibular signals improves heading discrimination in the presence of a moving object. *J Neurosci* 2015; 35(40): 13599–13607.
18. Dokka K, Park H, Jansen M, et al. Causal inference accounts for heading perception in the presence of object motion. *Proc Natl Acad Sci U S A* 2019; 116(18): 9060–9065.
19. Ramkhalawansingh R, Butler JS, and Campos JL. Visual-vestibular integration during self-motion perception in younger and older adults. *Psychol Aging* 2018; 33(5): 798–813.
20. Gallagher M, Choi R, and Ferrè ER. Multisensory interactions in virtual reality: optic flow reduces vestibular sensitivity, but only for congruent planes of motion. *Multisensory Res* 2020; 33(6): 625–644.
21. Rodriguez R and Crane BT. Common causation and offset effects in human visual-inertial heading direction integration. *J Neurophysiol* 2020; 123(4): 1369–1379.
22. Fetsch CR, Turner AH, DeAngelis GC, et al. Dynamic reweighting of visual and vestibular cues during self-motion perception. *J Neurosci* 2009; 29(49): 15601–15612.
23. Butler JS, Campos JL, Bülthoff HH, et al. The role of stereo vision in visual-vestibular integration. *Seeing Perceiving* 2011; 24(5): 453–470.
24. De Winkel KN, Weesie J, Werkhoven PJ, et al. Integration of visual and inertial cues in perceived heading of self-motion. *J Vis* 2010; 10(12): 1–10.
25. de Winkel KN, Katliar M, and Bülthoff HH. Forced fusion in multisensory heading estimation. *PLoS One* 2015; 10(5): e0127104.
26. Drugowitsch J, Moreno-Bote R, and Pouget A. Relation between belief and performance in perceptual decision making. *PLoS One* 2014; 9(5): e96511.
27. Gu Y, DeAngelis GC, and Angelaki DE. A functional link between area MSTd and heading perception based on vestibular signals. *Nat Neurosci* 2007; 10(8): 1038–1047.
28. Noel JP and Angelaki DE. Cognitive, systems, and computational neurosciences of the self in motion. *Annu Rev Psychol* 2022; 73: 103–129.
29. Fetsch CR, Pouget A, DeAngelis GC, et al. Neural correlates of reliability-based cue weighting during multisensory integration. *Nat Neurosci* 2012; 15(1): 146–154.
30. Palmer TD and Ramsey AK. The function of consciousness in multisensory integration. *Cognition* 2012; 125(3): 353–364.
31. Faivre N and Koch C. Temporal structure coding with and without awareness. *Cognition* 2014; 131(3): 404–414.
32. Mudrik L, Faivre N, and Koch C. Information integration without awareness. *Trends Cognit Sci* 2014; 18(9): 488–496.
33. Spence C. Multisensory perception. In: *Stevens' handbook of experimental psychology and cognitive neuroscience*. Hoboken, NJ: Wiley, 2018, Vol. 2, pp. 1–56.
34. Yu R. Unconscious integration: current evidence for integrative processing under subliminal conditions. *Br J Psychol* 2023; 114(2): 430–456.

35. Ngo MK and Spence C. Crossmodal facilitation of masked visual target identification. *Atten Percept Psychophys* 2010; 72(7): 1938–1947.
36. Rodriguez R and Crane BT. Effect of timing delay between visual and vestibular stimuli on heading perception. *J Neurophysiol* 2021; 126(1): 304–312.
37. Wei Y, Okazaki YO, So RH, et al. Motion sickness-susceptible participants exposed to coherent rotating dot patterns show excessive N2 amplitudes and impaired theta-band phase synchronization. *Neuroimage* 2019; 202: 116028.
38. Golding JF. Motion sickness susceptibility questionnaire revised and its relationship to other forms of sickness. *Brain Res Bull* 1998; 47(5): 507–516.
39. Fu XJ, Wei Y, Chen DJZ, et al. Interaction effect of frequency, velocity and amplitude on perceived vection magnitude for yaw visual oscillation. *J Vis* 2017; 17(10): 364.
40. So RHY, Wei Y, and Chen DJZ. Vection provoked by visual oscillation: is frequency the major determining factor? In: 2017 IEEE 6th Global Conference on Consumer Electronics (GCCE), Nagoya, 24–27 October 2017, pp. 1–2. IEEE.
41. De Bruyn B and Orban GA. The role of direction information in the perception of geometric optic flow components. *Percept Psychophys* 1990; 47(5): 433–438.
42. Ahlstrom U and Borjesson E. Segregation of motion structure from random visual noise. *Perception* 1996; 25(3): 279–292.
43. Kennedy RS, Lane NE, Berbaum KS, et al. Simulator sickness questionnaire: an enhanced method for quantifying simulator sickness. *Int J Aviat Psychol* 1993; 3(3): 203–220.
44. De Winkel KN, Soyka F, Barnett-Cowan M, et al. Integration of visual and inertial cues in the perception of angular self-motion. *Exp Brain Res* 2013; 231(2): 209–218.
45. Brandt T, Glasauer S, Stephan T, et al. Visual-vestibular and visuovisual cortical interaction: new insights from fMRI and pet. *Ann N Y Acad Sci* 2002; 956: 230–241.
46. Deutschla A, Bense S, Stephan T, et al. Sensory system interactions during simultaneous vestibular and visual stimulation in PET. *Hum Brain Mapp* 2002; 16: 92–103.
47. Seemungal BM, Guzman-Lopez J, Arshad Q, et al. Vestibular activation differentially modulates human early visual cortex and V5/MT excitability and response entropy. *Cerebr Cortex* 2013; 23(1): 12–19.
48. Della-Justina HM, Gamba HR, Lukasova K, et al. Interaction of brain areas of visual and vestibular simultaneous activity with fMRI. *Exp Brain Res* 2014; 233: 237–252.
49. Brandt T, Bartenstein P, Janek A, et al. Reciprocal inhibitory visual-vestibular interaction. Visual motion stimulation deactivates the parieto-insular vestibular cortex. *Brain* 1998; 121(9): 1749–1758.
50. He X and Bao M. Neuroimaging evidence of visual-vestibular interaction accounting for perceptual mislocalization induced by head rotation. *Neurophotonics* 2024; 11(1): 015005.
51. Öztürk ŞT, Şerbetçioğlu MB, Ersin K, et al. The impact of optical illusions on the vestibular system. *J Audiol Otol* 2021; 25(3): 152–158.